JOURNAL OF MATHEMATICAL PSYCHOLOGY 35, 411–442 (1991)

Texture Quilts: Basic Tools for Studying Motion-from-Texture

CHARLES CHUBB

Department of Psychology, Rutgers University

AND

GEORGE SPERLING

Psychology Department and Center for Neural Sciences, New York University

A theoretical foundation and concrete stimulus-construction methods are provided for studying motion-from-spatial-texture without contamination by motion mechanisms sensitive to other aspects of the signal. Specifically, examples are constructed of a special class of random stimuli called *texture quilts*. Although, as we demonstrate experimentally, certain texture quilts display consistent apparent motion, it is proven that their motion content (a) is unavailable to standard motion analysis (such as might be accomplished by an Adelson/Bergen motion-energy analyzer, a Watson/Ahumada motion sensor, or by any elaborated Reichardt detector), and (b) cannot be exposed to standard motion analysis by any purely temporal signal transformation no matter how nonlinear (e.g., temporal differentiation followed by rectification). Applying such a purely temporal transformation to any texture quilt produces a spatiotemporal function P whose motion is unavailable to standard motion analysis: The expected response of every Reichardt detector to P is 0 at every instant in time. The simplest mechanism sufficient to sense the motion exhibited by texture quilts consists of three successive stages: (i) a purely spatial linear filter, (ii) a rectifier (but not a perfect square law) to transform regions of large negative or positive responses into regions of high positive values, and (iii) standard motion analysis.

1. INTRODUCTION

Standard Motion Analysis. The extensive literature on the motion of random-dot cinematograms (Anstis, 1970; Baker & Braddick, 1982a, 1982b; Bell & Lappin, 1979; Braddick, 1973, 1974; Chang & Julesz, 1983a, 1983b, 1985; van Doorn & Koenderink, 1984; Julesz, 1971; Lappin & Bell, 1972; Nakayama & Silverman, 1984; Ramachandran & Anstis, 1983) points toward the view that a "short-range" system (Braddick, 1973, 1974) submits the raw spatiotemporal luminance function directly to *standard motion analysis* (such as might be accomplished by an Adelson/Bergen motion-energy detector (Adelson & Bergen, 1985), a Watson/Ahumada

Reprint requests should be sent to Charles Chubb, Department of Psychology, Rutgers University, New Brunswick, NJ 08903 or George Sperling, HIP Lab, NYU, 6 Washington Place, New York, NY 10003.

0022-2496/91 $3.00

motion sensor (Watson & Ahumada, 1983a, 1983b, 1985), an elaborated Reichardt detector (van Santen & Sperling, 1984, 1985), or some variants of a gradient detector (Marr & Ullman, 1981; Adelson & Bergen, 1986).

Fourier and Non-Fourier Mechanisms. An impressive number of observations suggest that standard motion analysis is not the whole story (Bowne, McKee, & Glaser, 1989; Cavanagh, Arguin, & von Grunau, 1989; Derrington & Badcock, 1985; Derrington & Henning, 1987; Green, 1986; Lelkins & Koenderink, 1984; Pantle & Turano, 1986; Petersik, Hicks, & Pantle, 1978; Ramachandran, Ginsburg, & Anstis, 1983; Ramachandran, Rao, & Vidyasagar, 1973; Sperling, 1976; Turano & Pantle, 1989). In particular, Chubb and Sperling (1987, 1988) have demonstrated a variety of stimuli that display consistent, unambiguous apparent motion, yet that do not systematically stimulate mechanisms that apply standard motion analysis directly to luminance. For reasons that become clear in Section 2, we call any motion system that applies standard analysis to the raw signal as a *Fourier* mechanism, and we refer to any system that applies standard analysis to a nonlinear transformation of the signal as a *non-Fourier* mechanism.

Microbalanced Stimuli. The methods used by Chubb & Sperling to construct stimuli whose obvious and consistent motion content cannot be revealed by applying standard motion analysis directly to luminance are founded on the notion of a *microbalanced* random stimulus. In Section 2.3.5, we show that the expected response of any standard motion analyzer applied directly to any microbalanced random stimulus is equal to the expected response of the corresponding analyzer tuned to motion of the same type, but in the opposite direction.

Microbalanced random stimuli allow us to differentially stimulate non-Fourier motion mechanisms without systematically engaging Fourier mechanisms. This is the source of their importance in the study of motion perception.

There are probably several types of non-Fourier motion mechanisms, distinguished by the different transformations they apply to the signal prior to standard motion analysis. In this paper, we extend the theory of microbalanced random stimuli in order to develop methods for constructing stimuli that selectively engage specific classes of non-Fourier mechanisms without stimulating either Fourier mechanisms or other classes of non-Fourier mechanisms.

Pointwise Transformations; Static Nonlinearities. A transformation T is called *pointwise* if the output of T at any point (x, y, t) in space-time depends only on the (stimulus) input value at that point. A *nonlinear* pointwise transformation sometimes is called a *static nonlinearity*. For instance, simple rectifiers and thresholders are pointwise transformations. In Section 3, we address the problem of isolating the class of non-Fourier mechanisms that apply a simple pointwise transformation prior to standard motion analysis from the class of all those mechanisms that apply more complicated transformations. The central result in this section is proposition 3.2 which provides necessary and sufficient conditions for a random stimulus I to be such that any pointwise transformation of I is microbalanced.

Purely Temporal Transformations and Texture Quilts. The results with pointwise transformations are extended in Section 4 to purely temporal transformations (defined in Section 2.2). Whereas, for a pointwise transformation, the transformed value at the point (x, y, t) depends only on the stimulus value at (x, y, t), in a purely temporal transformation the transformed value at (x, y, t) may depend in any way whatsoever on the entire history of stimulus values at (x, y). We define the class of stimuli called *texture quilts* (Definition 4.1) whose importance derives from the fact (proven in proposition 4.3) that any purely temporal transformation of a texture quilt is microbalanced. Concrete methods are provided for constructing *binary* and *sinusoidal* texture quilts that display consistent motion.

In Section 5, these construction methods are applied in an experiment designed to demonstrate the effectiveness of three textural properties as carriers of motion information. The textural properties are (i) spatial frequency variation, (ii) orientation variation, and (iii) variation between perceptually distinct textures with identical expected energy spectra.

2. Preliminaries

This section states the background facts presupposed by the main discussion of the paper.

2.1. *Discrete Dynamic Visual Stimuli*

Notation. Let $\mathbb{R}$ denote the real numbers, and $\mathbf{Z}$ ($\mathbf{Z}^+$) the integers (positive integers). We use square brackets to enclose arguments of discrete functions, and parentheses to enclose arguments of continuous functions.

The Range of a Stimulus. We want the term "stimulus" to refer not only to the luminance function submitted as input to the retina, but to any physiologically reasonable transformation of the spatiotemporal luminance function which might be submitted as input to a component processor of the visual system. Consequently, although luminance is physically a nonnegative quantity, we do not apply this constraint to the class of functions we admit as stimuli. We allow stimuli to take values throughout the positive and negative real numbers.

The Domain of a Stimulus. To remain close to our intuitions about neurally realized visual processors, we take stimuli to be a functions of the discrete domain $\mathbf{Z}^3$ (where the dimensions correspond to horizontal and vertical space, and time). In addition, for mathematical convenience, and without loss of physiological plausibility, we require a stimulus to be 0 almost everywhere in its (infinite) domain.

The Definition of a Stimulus. We call any function $I: \mathbf{Z}^3 \to \mathbb{R}$ a *stimulus* provided $I[x, y, t] = 0$ for all but finitely many points of $\mathbf{Z}^3$.

We shall be considering stimuli as functions of two spatial dimensions x, y and time t.

Stimulus Contrast. As is now well established (e.g., Shapley & Enroth-Cugell, 1984), early retinal gain-control mechanisms pass not stimulus luminance, but rather a signal approximating stimulus *contrast*, the normalized deviation at each time t of luminance at each point (x, y) in the visual field from a "background level," or "level of adaptation," which reflects the average luminance over points proximal to (x, y, t) in space and time. Because the transformation from luminance to contrast is a processing stage that is general to all of vision, we shall drop reference to mean luminance L_0, and characterize L only by its *contrast modulation function*, C:

$$C = \frac{L}{L_0} - 1. \tag{1}$$

What we argue in this paper is that the broad-band spatial filtering that mediates the step from luminance to contrast is succeeded by additional filtering stages in which a number of *narrowly tuned* spatial filters are applied to the visual signal, their output rectified, and the resulting spatiotemporal signal processed for motion information.

The History of a Stimulus at a Point in Space. For any stimulus I, any point $(x, y) \in \mathbf{Z}^2$, we define $I_{(x,y)}$, the *history of I at* (x, y), by setting

$$I_{(x,y)}[t] = I[x, y, t] \tag{2}$$

for all $t \in \mathbf{Z}$.

Space-Time Separable Stimuli. A stimulus I is called *space-time* separable iff I can be expressed as the product of a spatial function $f: \mathbf{Z}^2 \to \mathbb{R}$ and a temporal function $g: \mathbf{Z} \to \mathbb{R}$: For all $(x, y, t) \in \mathbf{Z}^3$, $I[x, y, t] = f[x, y]\, g[t]$.

The Fourier Transform of a Stimulus. Because any stimulus I is nonzero at only a finite number of points, the energy in I is finite, implying that I has a well-defined Fourier transform.

We denote I's Fourier transform by $\bar{I}$: writing j for the complex number (0, 1),

$$\bar{I}(\omega, \theta, \tau) = \sum_{x=-\infty}^{\infty} \sum_{y=-\infty}^{\infty} \sum_{t=-\infty}^{\infty} I[x, y, t]\, e^{-j(\omega x + \theta y + \tau t)}. \tag{3}$$

Although $\bar{I}$ is defined for all real numbers ω, θ, τ, it is periodic over 2π in each argument. This fact is reflected in the inverse transform:

$$I[x, y, t] = \frac{1}{(2\pi)^3} \int_0^{2\pi} \int_0^{2\pi} \int_0^{2\pi} \bar{I}(\omega, \theta, \tau)\, e^{j(\omega x + \theta y + \tau t)}\, d\omega\, d\theta\, d\tau. \tag{4}$$

In the Fourier domain, we consistently use ω to index frequencies relative to x, θ frequencies relative to y, and τ frequencies relative to t.

The Function **0**. We write **0** for any function that assigns 0 to each element in its domain. Thus, **0** defined on $\mathbf{Z}^3$ is the stimulus that is zero throughout space and time. We also write **0** for the temporal function that sets $\mathbf{0}[t] = 0$ for all $t \in \mathbf{Z}$.

2.2. *Mappings and Stimulus Transformations*

Let Ω be the set of all real-valued functions of $\mathbf{Z}^3$, and call any function of Ω into Ω a *mapping*. (We shall need the general notion of a mapping only briefly in order to specify the subset of well-behaved mappings called transformations.) For any mapping M and any $I \in \Omega$, $M(I)$ is a real-valued function of $\mathbf{Z}^3$; accordingly, we write $M(I)[x, y, t]$ for the value of $M(I)$ at any point $(x, y, t) \in \mathbf{Z}^3$.

If it is continuous, a function $f: \mathbb{R} \to \mathbb{R}$ submits to a wide range of useful operations. For instance, if f is continuous, it can be integrated over any finite interval. Of course, f need not be continuous to meet this condition. For instance, f is integrable over any finite interval if f is discontinuous at only a finite number of points in any finite interval. If f is integrable over any finite interval, and if f also is bounded, then for any function g for which $\int_{\mathbb{R}} g$ converges, $\int_{\mathbb{R}} fg$ also converges. In particular, $\int_{\mathbb{R}} fg$ converges if g is a density function. For the results reported here, we restrict our attention to a special class of mappings, which we shall call stimulus transformations, that have properties analogous to those of the well-behaved function f. We specify these desirable properties in the following paragraph.

Continuous Mappings; Finitely Integrable Mappings; Bounded Mappings. For any $I \in \Omega$, any $p \in \mathbb{R}$, any $\psi \in \mathbf{Z}^3$, we write $I_{\psi \leftarrow p}$ for the element of Ω that is identical to I at all locations of $\mathbf{Z}^3$ except ψ, where it takes the value p. Any mapping M is called *continuous* if $M(I_{\psi \leftarrow p})[\zeta]$ is a continuous function of p for any $I \in \Omega$, and any $\psi, \zeta \in \mathbf{Z}^3$. M is called *finitely integrable* if, for any such I, ψ, and ζ, $M(I_{\psi \leftarrow p})[\zeta]$ is an integrable function of p over any finite interval. Finally, M is called *bounded* if, for any such I, ψ, and ζ, $M(I_{\psi \leftarrow p})[\zeta]$ is a bounded function of p over the set of real numbers.

DEFINITION OF A STIMULUS TRANSFORMATION. A *stimulus transformation* (which we shall often refer to simply as a *transformation*) is a bounded, finitely integrable, mapping T such that $T(S)$ is a stimulus for any stimulus S, and $T(\mathbf{0}) = \mathbf{0}$.

There are other reasonable constraints we might impose on the notion of a stimulus transformation. For instance, we might require a stimulus transformation to be time-invariant and causal. However, we do not include these conditions in our definition because they are not required for the results we report.

Purely Temporal Stimulus Transformations. Let Ω_T be the set of all functions mapping $\mathbf{Z}$ into $\mathbb{R}$. A transformation H is called *purely temporal* iff there exists a function $H_T: \Omega_T \to \Omega_T$ such that for any stimulus I, any $(x, y, t) \in \mathbf{Z}^3$,

$$H(I)[x, y, t] = H_T(I_{(x, y)})[t]. \tag{5}$$

That is, the value at the point $(x, y, t) \in \mathbf{Z}^3$ that results from applying H to I depends only on the history of I at (x, y). Since it is obvious from the context, we drop the distinction between H and H_T, and allow H to be applied both to full-fledged stimuli and to simple functions of time. Thus, for any temporal function $P: \mathbf{Z} \to \mathbb{R}$, we shall write $H(P)$ to indicate the temporal function $H_T(P)$.

We shall be particularly concerned with two types of transformations: *pointwise* transformations and *linear, shift-invariant* transformations.

Pointwise Transformations and Rectifiers. For any functions $f: A \to B$ and $g: B \to C$, the *composition* $g \bullet f: A \to C$ is given by

$$g \bullet f(a) = g(f(a)) \tag{6}$$

for any $a \in A$. For any $f: \mathbb{R} \to \mathbb{R}$, we call the mapping $f\bullet$, yielding the spatiotemporal function $f \bullet I$ when applied to stimulus I, a *pointwise* mapping (because its output value at any point in space-time depends only on its input value at that point).

As is evident, $f\bullet$ is a transformation iff (i) $f(0) = 0$, (ii) f is bounded on $\mathbb{R}$, and (iii) f is integrable over any bounded real interval. A transformation $f\bullet$ is called a *positive half-wave rectifier* if f is monotonically increasing, and $f[v] = 0$ for all $v \leqslant 0$; $f\bullet$ is called a *negative half-wave rectifier* if f is monotonically decreasing, and $f[v] = 0$ for $v \geqslant 0$. Finally, $f\bullet$ is called a *full-wave rectifier* if f is a monotonically increasing function of absolute value.

Linear, Shift-Invariant (LSI) Transformations. For any offset $\psi \in \mathbf{Z}^3$, define the mapping S^ψ by

$$S^\psi(I)[\zeta] = I[\zeta - \psi] \tag{7}$$

for any $I \in \Omega$. Thus $S^\psi(I)$ is derived by shifting I by the offset ψ in $\mathbf{Z}^3$. Any mapping M is called *shift-invariant* iff

$$S^\psi(M(I)) = M(S^\psi(I)) \tag{8}$$

for any $\psi \in \mathbf{Z}^3$, any $I \in \Omega$. In addition, M is *linear* iff for any $I, J \in \Omega$, any real numbers κ and λ

$$M(\kappa I + \lambda J) = \kappa M(I) + \lambda M(J). \tag{9}$$

As is well known, any linear, shift-invariant (LSI) transformation can be expressed as a *convolution*, which is defined for any $u \in \mathbf{Z}^3$ by

$$(k * I)[u] = \sum_{v \in \mathbf{Z}^3} k[u - v]\, I[v], \tag{10}$$

for some $k: \mathbf{Z}^3 \to \mathbb{R}$. The function k is called the *impulse response* of the transformation $k*$.

2.3. *Random Stimuli*

For any real random variable X with density f, we write $E[X]$ for the *expectation of* X:

$$E[X] = \int_{\mathbb{R}} xf(x)\,dx. \tag{11}$$

The notion of a random stimulus generalizes that of a (nonrandom) stimulus in that the values assigned points in space-time by a random stimulus are random variables (with finite variances) rather than constants.

DEFINITION OF A RANDOM STIMULUS. Call any family $\{R[x, y, t] \| (x, y, t) \in \mathbf{Z}^3\}$ of jointly distributed random variables a *random stimulus* provided

(i) $R[x, y, t]$ is constant and equal to 0 for all but finitely many $(x, y, t) \in \mathbf{Z}^3$, and

(ii) $E[R[x, y, t]^2]$ exists for all $(x, y, t) \in \mathbf{Z}^3$.

As with nonrandom stimuli, we write $\bar{R}$ for the Fourier transform of any random stimulus R; and, for any $\chi = (x, y) \in \mathbf{Z}^2$ we write R_χ for the temporal random function defined by

$$R_\chi[t] = R[\chi, t] \tag{12}$$

for all times $t \in \mathbf{Z}$.

Space-Time Separable Random Stimuli. We call a random stimulus R *space-time separable* iff R is space-time separable with probability 1.

Constant Stimuli. Any ordinary stimulus can be regarded as a random stimulus that does not vary across independent realizations. We call such unvarying stimuli *constant*.

The Motion-from-Fourier-Components Principle. Parseval's relation states that the energy in a stimulus is proportional to the energy in its Fourier transform. Individual spatiotemporal Fourier components are drifting sinusoidal gratings. Thus, we can add up the energy in a dynamic visual stimulus either point-by-point in space-time, or drifting sinusoid by drifting sinusoid. A commonly encountered rule of thumb (van Santen & Sperling, 1985; Watson & Ahumada, 1983b; Watson, Ahumada, & Farrell, 1986) for predicting the apparent motion of an arbitrary stimulus $I[x, y, t] = f[x, t]$ (constant in the vertical dimension of space), is the *motion-from-Fourier-components* principle: For I regarded as a linear combination of drifting sinusoidal gratings, if most of I's energy is contributed by rightward-drifting gratings, then perceived motion should be to the right. If most of the energy resides in the leftward-drifting gratings, perceived motion should be to the left. Otherwise I should manifest no decisive motion in either direction.

Drift-Balanced Random Stimuli. The class of *drift-balanced* random stimuli (Chubb & Sperling, 1987, 1988) provides a rich pool of counterexamples to the motion-from-Fourier-components principle. A random stimulus R is drift balanced iff the expected energy in R of each drifting sinusoidal component is equal to the expected energy of the component of the same spatial frequency, drifting at the same rate, but in the opposite direction. The term *drift balanced* is defined formally as follows.

DEFINITION OF A DRIFT-BALANCED RANDOM STIMULUS. Call any random stimulus R *drift balanced* iff

$$E[|\bar{R}(\omega, \theta, \tau)|^2] = E[|\bar{R}(\omega, \theta, -\tau)|^2] \tag{13}$$

for all $(\omega, \theta, \tau) \in \mathbb{R}^3$.[1]

Thus, for any class of spatiotemporal linear receptors tuned to stimulus energy in a certain spatiotemporal frequency band, a drift-balanced random stimulus will, on the average, stimulate equally well those receptors tuned to the corresponding band of opposite temporal orientation.

Microbalanced Random Stimuli. Consider the following two-flash stimulus S: In flash 1, a bright spot (call it Spot 1) appears. In flash 2, Spot 1 disappears, and two new spots appear, one to the left and one symmetrically to the right of Spot 1. As one might suppose, S is drift balanced. On the other hand, it is equally clear that a Fourier motion detector whose spatial reach encompasses the location of Spot 1 and only *one* of the Spots in flash 2 may well be stimulated in a fixed direction by S. Thus, although S is drift balanced, some Fourier motion detectors may be stimulated strongly and systematically by S. These detectors can be differentially selected by *spatial windowing*, and thereby the drift-balanced stimulus S is converted into a non-drift-balanced stimulus by multiplying it by an appropriate space-time separable function. The following subclass of drift-balanced random stimuli cannot be made non-drift-balanced by space-time separable windowing.

DEFINITION OF A MICROBALANCED RANDOM STIMULUS. Call any random stimulus I *microbalanced* iff the product WI is drift balanced for any space-time separable function W.

One can think of the multiplying function W as a "window" through which a spatiotemporal subregion of I can be "viewed" in isolation. The space-time separability of W ensures that W is "transparent" with respect to the motion-content of the region to which it is applied: W does not distort I's motion with any motion content of its own. The fact that I is microbalanced means that any subregion of I encountered through a "motion-transparent window" is drift balanced.

[1] For a proof that the expected energy of the Fourier transform of any random stimulus is everywhere well defined see Chubb & Sperling (1988, Appendix A).

The following characterization of the class of microbalanced random stimuli, and all other results stated without proof in this section, are from Chubb and Sperling (1988).

2.3.1. *A random stimulus I is microbalanced if and only if*

$$E[I[x, y, t]\, I[x', y', t'] - I[x, y, t']\, I[x', y', t]] = 0 \tag{14}$$

for all $x, y, t, x', y', t' \in \mathbf{Z}$.

Some other relevant facts about microbalanced random stimuli:

2.3.2. *For any independent microbalanced random stimuli I and J,*

I. *the product IJ is microbalanced,*

and

II. *the convolution $I * J$ is microbalanced.*

2.3.3. (a) *Any space-time separable random stimulus is microbalanced*; (b) *any constant microbalanced stimulus is space-time separable.*

The following result is useful in constructing a wide range of microbalanced random stimuli which display striking apparent motion.

2.3.4. *Let Γ be a family of pairwise independent, microbalanced random stimuli, all but at most one of which have expectation* **0**. *Then any linear combination of Γ is microbalanced.*

Reichardt Detectors and Microbalanced Random Stimuli. Two Fourier motion detectors proposed for psychophysical data (Adelson & Bergen, 1985; Watson & Ahumada, 1983a, 1983b) can be recast as *Reichardt detectors* (Adelson & Bergen, 1985; van Santen & Sperling, 1985). The Reichardt detector has many useful properties as a motion detector without regard to its specific instantiation (van Santen & Sperling, 1984, 1985).

Figure 1 shows a diagram of the Reichardt detector. It consists of spatial receptors characterized by spatial functions f_1 and f_2, temporal filters g_1* and g_2*, multipliers, a differencer, and another temporal filter $h*$. The spatial receptors f_i, $i = 1, 2$, act on the input stimulus I to produce intermediate outputs,

$$y_i[t] = \sum_{(x, y) \in \mathbf{Z}^2} f_i[x, y]\, I[x, y, t]. \tag{15}$$

At the next stage, each temporal filter g_j* transforms its input y_i $(i, j = 1, 2)$, yielding four temporal output functions: $g_j * y_i$. The left and right multipliers then compute the products

$$[y_1 * g_1[t]][y_2 * g_2[t]] \quad \text{and} \quad [y_1 * g_2[t]][y_2 * g_1[t]], \tag{16}$$

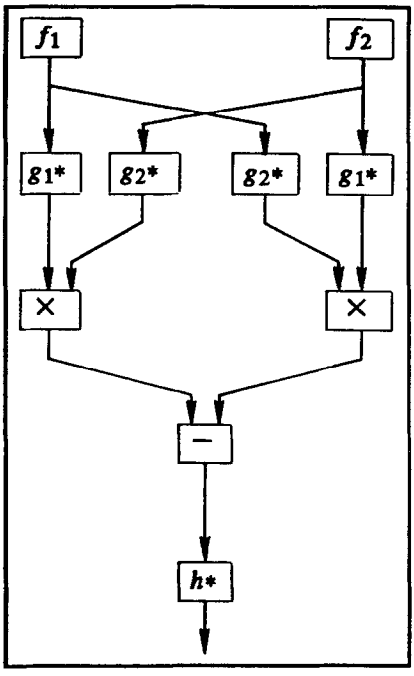

FIG. 1. The Reichardt detector. Let I be a random stimulus. Then, in response to I, for $i = 1, 2$, the box containing the spatial function $f_i: \mathbf{Z}^2 \rightarrow \mathbb{R}$, outputs the temporal function, $\sum_{(x,y)\in \mathbf{Z}^2} f_i[x, y]\, I[x, y, t]$; each of the boxes marked g_i* outputs the convolution of its input with the temporal function $g_i: \mathbf{Z} \rightarrow \mathbb{R}$; each of the boxes marked with a multiplication sign outputs the product of its inputs; the box marked with a minus sign outputs its left input minus its right; and the box containing $h*$ outputs the convolution of its input with the temporal function $h: \mathbf{Z} \rightarrow \mathbb{R}$. To see how the Reichardt detector senses motion, suppose f_2 is identical to f_1, but shifted in space by some offset, and suppose the filters g_1* do not alter their input, while the filters g_2* simply delay their input by some amount δ_t of time. Then a rigidly translating pattern moving in the direction of box f_2's offset from box f_1 will elicit some time-varying response from box f_1, and the same response a short time later from box f_2. If that "short time later" is precisely δ_t, the output of the righthand multiplier will be positive as long as the pattern keeps drifting. This will result in a net negative Reichardt detector output. If the pattern drift is in the opposite direction, the detector response will be positive.

respectively, and the differencer subtracts the output from the right multiplier from that of the left multiplier:

$$D[t] = [y_1 * g_1[t]][y_2 * g_2[t]] - [y_1 * g_2[t]][y_2 * g_1[t]]. \tag{17}$$

The final output is produced by applying the filter $h*$, whose purpose is to smooth the time-varying, differencer output D. Since many Fourier mechanisms can be expressed as, or closely approximated by, Reichardt detectors (Adelson & Bergen, 1985, 1986; van Santen & Sperling, 1985), the following characterization of the class of microbalanced stimuli can be regarded as the cornerstone of the claim that microbalanced random stimuli bypass Fourier motion mechanisms.

2.3.5. *For any random stimulus I, the following conditions are equivalent:*

(I) *I is microbalanced.*

(II) *The expected response of every Reichardt detector to I is* 0 *at every instant in time.*

Proof. Chubb & Sperling (1988) proved that I implies II. To obtain the reverse implication, note that if II holds, then, in particular, for any points (x, y), $(x', y') \in \mathbf{Z}^2$ and any $\delta_t \in \mathbf{Z}$, the expected response to I is the temporal function $\mathbf{0}$ for a particular simple Reichardt detector that computes

$$I[x, y, t]\, I[x', y', t-\delta_t] - I[x, y, t-\delta_t]\, I[x', y', t]. \tag{18}$$

This Reichardt detector is constructed by making (i) f_1 (of Fig. 1) the function that takes the value 1 at (x, y) and 0 everywhere else, (ii) f_2 the function that takes the value 1 at (x', y') and 0 everywhere else, (iii) each of g_1* and $h*$ the identity transformation, and (iv) g_2* the filter that delays its input by δ_t units of time. However, if the expected response to I is 0 throughout time for any such Reichardt detector, then Eq. (14) holds, and proposition 2.3.1 implies that I is microbalanced. ∎

3. Random Stimuli Microbalanced under All Pointwise Transformations

The main purpose of this paper is to provide tools for differentially stimulating specific types of non-Fourier motion mechanisms without engaging either Fourier mechanisms or other types of non-Fourier mechanisms. A non-Fourier motion mechanism is one that applies an initial nonlinear transformation to the visual signal and subjects the output to standard motion analysis. In this section, we provide some results relevant to the psychophysical problem of stimulating non-Fourier mechanisms whose initial transformation is nonpointwise without engaging any mechanism whose initial transformation is pointwise. The main finding is stated in proposition 3.2, which provides necessary and sufficient conditions for a random stimulus I to be such that $f \bullet I$ is microbalanced for any pointwise transformation $f\bullet$. In Section 4 we apply this result to construct random stimuli (texture quilts) which are microbalanced, and are, moreover, guaranteed to remain microbalanced after any purely temporal transformation. Such stimuli are useful for selectively stimulating non-Fourier motion mechanisms that extract motion information from stimuli that have undergone nonlinear *spatial* stimulus transformations.

We begin by considering an example of a stimulus (Chubb & Sperling, 1987, 1988) that is microbalanced under all pointwise transformations, but whose motion can be revealed by a purely temporal nonlinear transformation.

3.1. *Stimulus J: Traveling Reversal of a Random Black-or-White Vertical Bar Pattern.* Let $M \in \mathbf{Z}^+$. We construct the random stimulus J of $M+1$ frames

indexed 0, 1, ..., M, each of which contains M vertical bars, indexed 1, 2, ..., M from left to right. In frame 0 of stimulus J, all M vertical bars first appear. The contrast of each bar is 1 or -1 with equal probability, and bar contrasts are jointly independent. In each successive frame m, $m = 1, 2, ..., M$, the mth rectangle flips its contrast to 1 if its previous contrast was -1; otherwise it flips from 1 to -1. In frame 1, rectangle 1 flips contrast; in frame 2, rectangle 2 flips, and in successive frames, successive rectangles flip contrast from left to right, until the Mth rectangle flips in frame M, after which all the rectangles turn off. An xt cross-section of frames 0 to M of J is shown in Fig. 2a.

The traveling contrast-reversal, stimulus J, is easily expressed as a sum of pairwise independent, space-time separable random stimuli, all with expectation $\mathbf{0}$; thus propositions 2.3.3a and 2.3.4 imply that J is microbalanced. Moreover, it is easy to see that, because J's frames are comprised of only two values, any pointwise transformation of J merely serves to rescale each of J's frames, and to shift it by a constant: that is, for any $f: \mathbb{R} \to \mathbb{R}$, $f \bullet J = \lambda J + K$, where $\lambda \in \mathbb{R}$, and K is a stimulus

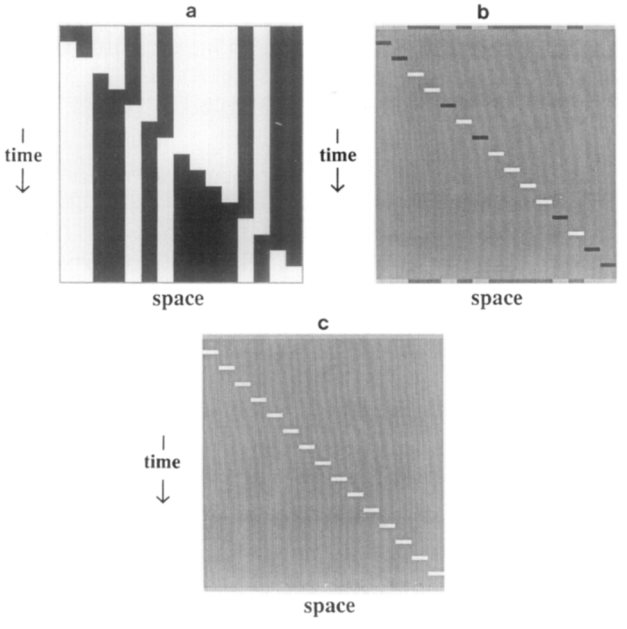

FIG. 2. Exposing the motion of the traveling contrast-reversal of the random black-or-white vertical bar pattern J to standard motion-analysis. (a) An xt cross-section of J. (b) An xt cross-section of the partial derivative of J with respect to time. (c) An xt cross-section of $|\partial J/\partial t|$. Each of J and $\partial J/\partial t$ is microbalanced. However, $|\partial J/\partial t|$ is not. In particular, $|\partial J/\partial t|$ has most of its energy at those frequencies whose velocity is equal to the velocity of the traveling contrast-reversal.

that assigns a constant value across all points at which J is nonzero. Clearly, $f \bullet J$ is another microbalanced random function (this follows easily from proposition 2.3.4). Thus, pointwise transformations fail to expose J's motion.

Exposing J's Motion to Standard Analysis. Perhaps the simplest way to extract J's motion is to full-wave rectify the partial derivative of J taken with respect to time. The stages of this transformation are illustrated in Figs. 2b and 2c. Figure 2b shows $\partial J/\partial t$. This function is itself microbalanced (propositions 2.3.2II and 2.3.3a imply that any purely temporal LSI transformation of a microbalanced random stimulus is microbalanced). However, $|\partial J/\partial t|$ (Fig. 2c) has most of its energy at those spatiotemporal frequencies whose velocity is equal to the velocity of the traveling contrast-reversal whose motion we wish to detect. Thus we see that, although J's motion cannot be exposed to standard analysis by a simple pointwise transformation, a temporal linear filter followed by a pointwise nonlinearity does suffice.

We turn now to the problem of stipulating the general conditions that a random stimulus I must satisfy so that $f \bullet I$ will be microbalanced for any pointwise transformation $f\bullet$. Call any random stimulus I *microbalanced under* a given transformation T iff $T(I)$ is microbalanced.

We state the following basic proposition (3.2) and its subsequent corollary (3.3) for continuously distributed random stimuli. The corresponding result for discretely distributed random stimuli is simpler and should be evident.

3.2. NECESSARY AND SUFFICIENT CONDITIONS FOR A RANDOM STIMULUS TO BE MICROBALANCED UNDER ALL POINTWISE TRANSFORMATIONS. *Let I be a random stimulus such that for any (x, y, t), $(x', y', t') \in \mathbf{Z}^3$, $(I[x, y, t], I[x', y', t'])$ has a continuous joint density. Then the following conditions are equivalent:*

(1) *I is microbalanced under all pointwise transformations.*

(2) *For all $x, y, t, x', y', t' \in \mathbf{Z}$, the joint density f of $(I[x, y, t], I[x', y', t'])$ and the joint density g of $(I[x, y, t'], I[x', y', t])$ satisfy*

$$f(p, q) + f(q, p) = g(p, q) + g(q, p) \tag{19}$$

for any $p, q \in \mathbb{R}$ such that $p \neq 0$ and $q \neq 0$.

Proof. Set $\kappa = I[x, y, t]$, $\lambda = I[x', y', t']$, $\gamma = I[x, y, t']$, and $\nu = I[x', y', t]$. Thus, (κ, λ) is distributed in $\mathbb{R}^2$ with density f and (γ, ν) is distributed with density g.

((2) implies (1)): By definition of any pointwise transformation $h\bullet$, we have $h(0) = 0$. Thus we need integrate only over values of κ and λ which are both nonzero in computing the expectation $E[h(\kappa)\, h(\lambda)]$. In particular, if Eq. (19) is satisfied for all $p \neq 0$ and $q \neq 0$, then $h \bullet I$ is microbalanced since

$$E[h(\kappa)\,h(\lambda)] = \frac{1}{2}\left[\int_{\mathbb{R}}\int_{\mathbb{R}} h(p)\,h(q)\,f(p,q)\,dp\,dq + \int_{\mathbb{R}}\int_{\mathbb{R}} h(q)\,h(p)\,f(q,p)\,dq\,dp\right]$$

$$= \frac{1}{2}\left[\int_{\mathbb{R}}\int_{\mathbb{R}} h(p)\,h(q)\,f(p,q)\,dp\,dq + \int_{\mathbb{R}}\int_{\mathbb{R}} h(p)\,h(q)\,f(q,p)\,dp\,dq\right]$$

$$= \frac{1}{2}\int_{\mathbb{R}}\int_{\mathbb{R}} h(p)\,h(q)(f(p,q)+f(q,p))\,dp\,dq$$

$$= \frac{1}{2}\int_{\mathbb{R}}\int_{\mathbb{R}} h(p)\,h(q)(g(p,q)+g(q,p))\,dp\,dq = E[h(\gamma)\,h(\nu)]. \quad (20)$$

(Note: the boundedness and finite integrability of $h\bullet$ ensure that these expectations exist.)

(Not (2) implies not (1)): On the other hand, suppose Eq. (19) fails for some $x, y, t, x', y', t' \in \mathbf{Z}$. One way in which this might happen is if $f(r,r) > g(r,r)$ for some nonzero $r \in \mathbb{R}$. In this case, there exists a neighborhood N of r, not including 0, such that $f(m,n) > g(m,n)$ for all $m, n \in N$. Thus, for the function $h: \mathbb{R} \to \mathbb{R}$ defined by

$$h(n) = \begin{cases} 1 & \text{if } n \in N, \\ 0 & \text{otherwise,} \end{cases} \quad (21)$$

$h\bullet$ is a pointwise transformation (the function h is bounded on $\mathbb{R}$, finitely integrable, and $h(0)=0$). However, $h\bullet I$ is not microbalanced since

$$E[h(\kappa)\,h(\lambda)] = \int_N\int_N f(m,n)\,dm\,dn > \int_N\int_N g(m,n)\,dm\,dn = E[h(\gamma)\,h(\nu)]. \quad (22)$$

To recapitulate, if Condition 2 fails because there exists a nonzero $r \in \mathbb{R}$ for which $f(r,r) \neq g(r,r)$, then Condition 1 fails (I is not microbalanced under all pointwise transformations).

The only other way in which Condition 2 can fail is if $f(r,r) = g(r,r)$ for all $r \neq 0$ in $\mathbb{R}$, but for some $p, q \in \mathbb{R}$, with neither p nor q equal to 0, $f(p,q)+f(q,p) > g(p,q)+g(q,p)$. In this case, we obtain disjoint neighborhoods M of p and N of q, neither including 0, such that

$$f(m,n)+f(n,m) > g(m,n)+g(n,m) \quad (23)$$

for all $m \in M$, $n \in N$; consequently,

$$\int_M \int_N f(m, n) + f(n, m)\, dm\, dn > \int_M \int_N g(m, n) + g(n, m)\, dm\, dn. \tag{24}$$

Moreover, since—by assumption—$f(p, p) = g(p, p)$ and $f(q, q) = g(q, q)$, we can tailor the neighborhoods M and N to make the difference

$$\left[\int_M \int_M f(m, m')\, dm\, dm' + \int_N \int_N f(n, n')\, dn\, dn'\right] - \left[\int_M \int_M g(m, m')\, dm\, dm' + \int_N \int_N g(n, n')\, dn\, dn'\right] \tag{25}$$

as small as we want. Consider, then, the function $h: \mathbb{R} \to \mathbb{R}$ defined by

$$h(u) = \begin{cases} 1 & \text{if } u \in M \cup N, \\ 0 & \text{otherwise.} \end{cases} \tag{26}$$

Again, $h\bullet$ is a pointwise transformation. However, $h \bullet I$ fails again to be microbalanced because, for suitably tailored M and N,

$$\begin{aligned} E[h(\kappa)\, h(\lambda)] &= \int_M \int_M f(u, v)\, du\, dv + \int_N \int_N f(u, v)\, du\, dv \\ &\quad + \int_M \int_N f(u, v) + f(v, u)\, du\, dv \\ &> \int_M \int_M g(u, v)\, du\, dv + \int_N \int_N g(u, v)\, du\, dv \\ &\quad + \int_M \int_N g(u, v) + g(v, u)\, du\, dv = E[h(\gamma)\, h(v)]. \quad \blacksquare \end{aligned} \tag{27}$$

3.3. COROLLARY. *Let I be a random stimulus such that for all (x, y, t), $(x', y', t') \in \mathbf{Z}^3$, the pair $(I[x, y, t], I[x', y', t'])$ has a continuous joint density. Then I is microbalanced under all pointwise transformations if the following condition holds for all $x, y, t, x', y', t' \in \mathbf{Z}$: For f the joint density of $(I[x, y, t], I[x', y', t'])$, and g the joint density of $(I[x, y, t'], I[x', y', t])$, either*

$$f(p, q) = g(p, q) \qquad \text{for all } p, q \in \mathbb{R},\ p \neq 0,\ q \neq 0, \tag{28}$$

or

$$f(p, q) = g(q, p) \qquad \text{for all } p, q \in \mathbb{R},\ p \neq 0,\ q \neq 0. \tag{29}$$

Proof. If Eq. (28) holds for some (x, y, t), $(x', y', t') \in \mathbf{Z}^3$, then we also have

$$f(q, p) = g(q, p) \qquad \text{for all } p, q \in \mathbb{R},\ p \neq 0,\ q \neq 0, \tag{30}$$

and we obtain Eq. (19) by adding Eq. (28) and Eq. (30). The same reasoning applies for Eq. (29). ∎

A random stimulus microbalanced under all pointwise transformations, but quite different from J of example 3.1 is the following, suggested by J. Lappin (1989).

3.4. *Stimulus K: Rotating Random-Dot Cylinder.* Construct K by taking the parallel projection of a set of points on (and/or inside) the surface of a cylinder rotating around a vertical axis. Let the contrast values of the points be independent, identically distributed random variables. As is well known, when properly constructed, K can display a very strong kinetic depth effect, with dots moving in one direction seen as being in the front of the axis of rotation, and dots moving in the other direction seen as being in the back (Dosher, Landy, & Sperling, 1989; Ullman, 1979). Nonetheless, K is microbalanced under all pointwise transformations: All of K's systematic motion is horizontal; thus, we can drop reference to y, and note that for any x, t, x', t', the joint distribution of $(K[x, t], K[x', t'])$ is identical to that of $(K[x, t'], K[x', t])$. Hence, by Corollary 3.3, Condition 3, K is microbalanced under all pointwise transformations.

4. Texture Quilts

The rest of this paper is devoted to illustrating how the results of Section 3 can be applied to construct stimuli which display consistent apparent motion that cannot be exposed to standard analysis by any purely temporal transformation. Specifically, we demonstrate several motion-displaying stimuli, called *texture quilts* (Definition 4.1), that are microbalanced under all purely temporal transformations.

As illustrated in Fig. 3, the simplest transformations that suffice to expose the motion of texture quilts to standard analysis involve a purely spatial linear filter $s*$ followed by a rectifier $r\bullet$:

$$T(Q) = r\bullet(s * Q). \tag{31}$$

The spatial filter $s*$ will respond with varying energy throughout regions of the visual field, depending on whether or not the textures to which it is tuned populate those regions. However, the output of a linear filter to a texture is positive or negative depending on the local phase of the texture. The purpose of rectification is to transform regions of high-variance $s*$ response into regions of high average value, thus ensuring that the rectified output registers the presence or absence of texture, independent of phase. The result $T(Q)$ is a spatiotemporal function whose value reflects the local texture preferences of $s*$ in the visual field as a function of time (Bergen & Adelson, 1988; Caelli, 1985).[2]

[2] In general, a spatial linear filter followed by a pointwise nonlinearity can have arbitrarily high order Volterra kernels, depending on the order of the Taylor series of the pointwise transformation. However, if we take the rectifier of step (2) to be $\text{Rect}(x) = x^2$, then this squared output of a spatial filter is a second order spatial transformation. Standard motion analysis is yet another second order transformation. Thus, when we subject the squared filter output to standard motion analysis, we are applying a fourth order operator.

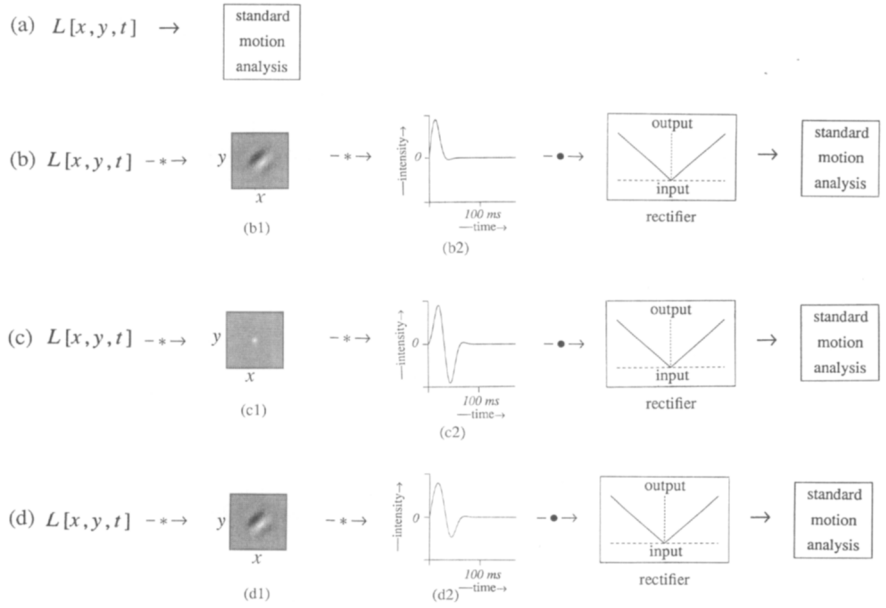

FIG. 3. Fourier and non-Fourier motion mechanisms. (a) Fourier motion mechanisms apply standard motion-analysis directly to the luminance signal L. (b), (c), and (d) Non-Fourier mechanisms apply standard motion-analysis to a nonlinear transformation of luminance. (b) A simple non-Fourier mechanism applies a signal transformation comprised of a spatiotemporal linear filter, followed by a pointwise nonlinearity. The $*$'s indicate spatial and temporal convolution, respectively, and $\bullet$ indicates function composition. The filtering performed in (b) is roughly pointwise in time (the temporal impulse response b2 approximates an impulse), and the nonlinearity applied is a full-wave rectifier. This system (with appropriately chosen spatial filter, b1) will extract the motion of the texture quilts shown in Figs. 4b, 5d, 6c, and 6d. It will not extract the motion of stimulus J, the traveling contrast-reversal of the random vertical bar pattern shown in Fig. 2a. (c) A spatially pointwise (the spatial impulse response c1 approximates an impulse), system with a flicker-sensitive temporal filter and a full-wave rectifier. Because of the flicker sensitivity, this mechanism will extract the motion of the traveling contrast-reversal of the random vertical bar pattern shown in Fig. 2a but not the motion of the texture quilts shown in Figs. 4b, 5d, 6c, and 6d. (d) The temporal filter d2 averages the temporal filters b2 and c2, and the pointwise nonlinearity is a full-wave rectifier. With an appropriate spatial filter d1, the non-Fourier system extracts the motion of any corresponding texture quilt as well as the motion of the traveling contrast-reversal of the random vertical bar pattern shown in Fig. 2a. However, it would be less well suited to these tasks than the detectors shown in (b) and (c) whose temporal filters it averages.

The essential trick in all the quilt examples we consider is to patch together various brief displays of static, random texture, taking appropriate measures to ensure that the resultant stimulus satisfies the following definition.

4.1. DEFINITION OF A TEXTURE QUILT. Let $A \subset \mathbf{Z}^2$ be a set of points in space, and let $t_0, t_1, ..., t_N$ be a strictly increasing sequence of times, with $T = \{t \| t_0 \leqslant t < t_N\}$. Call any random stimulus Q satisfying the following conditions a *texture quilt*:

(i) Q assigns 0 to all points outside $A \times T$.

(ii) For $i = 0, 1, ..., N-1$, the random values assigned by Q to points in A at time t_i remain unchanged until time t_{i+1}.

(iii) *Independence.* For $i = 0, 1, ..., N-1$, the random substimuli Q^i, defined, for all points α in space and all times t, by

$$Q^i[\alpha, t] = \begin{cases} Q[\alpha, t] & t_i \leqslant t < t_{i+1}, \alpha \in A \\ 0 & \text{otherwise,} \end{cases} \tag{32}$$

are jointly independent.

(iv) *Symmetry.* For any $\alpha, \beta \in A$, and any $t \in T$, the joint distribution of $(Q[\alpha, t], Q[\beta, t])$ is identical to the joint distribution of $(Q[\beta, t], Q[\alpha, t])$.

Terminology. Call A and T respectively Q's *spatial* and *temporal regions of activity*, and for $i = 0, 1, ..., N-1$, call $\{t \| t_i \leqslant t < t_{i+1}\}$ the ith *timeblock* of Q.

The empirical usefulness of texture quilts derives from proposition 4.3 in conjunction with the fact that it is easy to construct various sorts of texture quilts which display consistent apparent motion across independent realizations. The proof of proposition 4.3 is eased by the following

4.2. LEMMA. *Let Q be a texture quilt with spatial region of activity A. Then for any $\alpha, \beta \in A$, the pair of temporal functions (Q_α, Q_β) is distributed identically to the reverse pair (Q_β, Q_α).*

Proof. From Definition 4.1(i) and (ii), note that for temporal functions P and R, the density of the joint assignment $(Q_\alpha, Q_\beta) = (P, R)$ is 0 unless each of P and R is constant throughout each time block, and 0 outside T. Thus, any P and R for which the joint assignment $(Q_\alpha, Q_\beta) = (P, R)$ has nonzero density are completely determined by the values $P[t_i] = p_i$, and $R[t_i] = r_i$, for $i = 0, 1, ..., N-1$; for f_i the joint density of $(Q_\alpha[t_i], Q_\beta[t_i])$, Definition 4.1(iii) thus implies that the density of the joint assignment $(Q_\alpha, Q_\beta) = (P, R)$ is

$$\prod_{i=0}^{N-1} f_i(p_i, r_i). \tag{33}$$

But by Definition 4.1(iv), the quantity (33) is equal to

$$\prod_{i=0}^{N-1} f_i(r_i, p_i), \tag{34}$$

which is the density of the reverse occurrence that $(Q_\beta, Q_\alpha) = (P, R)$. ∎

4.3. TEXTURE QUILTS ARE MICROBALANCED UNDER PURELY TEMPORAL TRANSFORMATIONS. I. *Any texture quilt with a continuous joint density is microbalanced under all purely temporal, continuous transformations.*

II. *Any discretely distributed texture quilt is microbalanced under all purely temporal transformations.*

Proof of I. Let Q be a texture quilt with a continuous joint density, and let Φ be an arbitrary purely temporal, continuous transformation. We must prove that $\Phi(Q)$ is microbalanced. We can, of course, accomplish this by proving that $\Phi(Q)$ is microbalanced under all pointwise transformations (since, in particular, the identity transformation is pointwise). This turns out to be a convenient approach.

Let α, β be points in space, and let t and u be points in time. Because Φ is bounded and continuous and Q has a continuous joint density, we know that the joint density f of $(\Phi(Q)[\alpha, t], \Phi(Q)[\beta, u])$ and the joint density g of $(\Phi(Q)[\beta, t], \Phi(Q)[\alpha, u])$ both exist and are continuous on $\mathbb{R}^2$. We shall show for any $(p, r) \in \mathbb{R}^2$ with neither p nor r equal to 0, that either $f(p, r) = g(p, r)$ or $f(p, r) = g(r, p)$. The proposition will then follow from Corollary 3.3.

Case 1. At least one of α or β is outside A. Suppose α is outside A. Then by Definition 4.1(i), $Q_\alpha = \mathbf{0}$; hence $\Phi(Q)[\alpha, t] = \Phi(Q)[\alpha, u] = 0$. Consequently, $f(p, r) = g(r, p) = 0$ whenever $p \neq 0$. Thus Eq. (29) holds vacuously, with

$$f(p, r) = g(r, p) = 0 \qquad \text{for all } p, r \in \mathbb{R},\ p \neq 0,\ r \neq 0. \tag{35}$$

Case 2. Both α and β are in A. Let F be the joint density of (Q_α, Q_β) and G be the joint density of (Q_β, Q_α). By Lemma 4.2, $F = G$. Clearly, then, for F_Φ the joint density of $(\Phi(Q_\alpha), \Phi(Q_\beta))$ and G_Φ the joint density of $(\Phi(Q_\beta), \Phi(Q_\alpha))$, it follows that $F_\Phi = G_\Phi$. For any $p, r \in \mathbb{R}$, recall that $f(p, r)$ is the density of the co-occurrence that $\Phi(Q)[\alpha, t] = p$, and $\Phi(Q)[\beta, u] = r$, but this is precisely the density of the event that $(\Phi(Q_\alpha)[t], \Phi(Q_\beta)[u]) = (p, r)$. This density, however, is equal to the integral of F_Φ over all pairs of temporal functions (P, R) such that $P[t] = p$ and $R[u] = r$. Similarly, $g(p, r)$ is the density of the co-occurrence that $\Phi(Q)[\beta, t] = p$, and $\Phi(Q)[\alpha, u] = r$, but this is the density of the event that $(\Phi(Q_\beta)[t], \Phi(Q_\alpha)[u]) = (p, r)$, which is equal to the integral of G_Φ over all pairs of temporal functions (P, R) such that $P[t] = p$ and $R[u] = r$. However, as we have already noted, $F_\Phi = G_\Phi$, implying that $f = g$. Apply Corollary 3.3 to complete the proof. ∎

The proof of II is similar.

The rest of Section 4 is devoted to showing how to construct two kinds of simple texture quilts. In Section 5, we apply these construction techniques in an experiment to investigate what sorts of textural characteristics are actually processed for motion information by the visual system.

4.4. *Binary Texture Quilts*

4.4.1. *A General Technique for Constructing Binary Texture Quilts.* The simplest sorts of texture quilts involve only two contrast values. As in Definition 4.1, let $T = \{t \,\|\, t_0 \leqslant t < t_N\}$ be the temporal region of activity, with new timeblocks beginning at times $t_0, t_1, \ldots, t_{N-1}$. Let A be the spatial region of activity. Associate

with timeblocks $i=0, 1, ..., N-1$ spatial functions f_i (called *timeblock pictures*), each of which is 0 everywhere outside A, and takes only the values 1 and -1 within A. In addition, associate with timeblocks 0 through $N-1$ a family

$$\phi_0, \phi_1, ..., \phi_{N-1} \tag{36}$$

of jointly independent random variables, each of which takes the value 1 or -1 with equal probability. Then, for $i=0, 1, ..., N-1$, set

$$B_i[x, y, t] = \begin{cases} f_i[x, y] & \text{if } t \text{ is in timeblock } i, \\ 0 & \text{otherwise,} \end{cases} \tag{37}$$

and construct the random stimulus

$$B = \phi_0 B_0 + \phi_1 B_1 + \cdots + \phi_{N-1} B_{N-1}. \tag{38}$$

It is easy to see that B is a texture quilt. First, the functions B_i are defined to satisfy Definition 4.1(i) and (ii). The joint independence of the random variables ϕ_i ensures that B satisfies Definition 4.1(iii). To see that Definition 4.1(iv) is satisfied, note that for any $\alpha, \beta \in A$, either (i) $B_i[\alpha, t_i] = B_i[\beta, t_i]$ or (ii) $B_i[\alpha, t_i] = -B_i[\beta, t_i]$. In case (i),

$$B[\alpha, t_i] = \phi_i B_i[\alpha, t_i] = \phi_i B_i[\beta, t_i] = B[\beta, t_i], \tag{39}$$

implying that the pair $(B[\alpha, t_i], B[\beta, t_i])$ is distributed identically to the pair $(B[\beta, t_i], B[\alpha, t_i])$ (each pair with an equal probability of taking the value $(1, 1)$ or $(-1, -1)$). In case (ii)

$$B[\alpha, t_i] = -B[\beta, t_i], \tag{40}$$

and the pair $(B[\alpha, t_i], B[\beta, t_i])$ is distributed identically to the pair $(B[\beta, t_i], B[\alpha, t_i])$, each with an equal probability of assuming the value $(1, -1)$ or $(-1, 1)$. Thus Definition 4.1(iv) is satisfied along with 4.1(i), (ii), and (iii).

4.4.2. *Stimulus: The Sidestepping, Randomly Contrast-Reversing, Vertical Edge.* In Fig. 4b are displayed the 9 timeblock pictures comprising a particularly simple binary texture quilt. Note that the vertical dimension of Fig. 4b combines time and vertical space, precisely as a strip of movie film, scanned vertically, combines time and space. Timeblock pictures are separated by gray lines. Figure 4a shows the timeblock pictures f_0 through f_8 used in the construction, f_0 assigns the value -1 to all points (x, y) of the horizontal rectangle comprising the spatial region of activity, A. f_1 assigns 1 to the points in the leftmost eighth of A, and -1 to the points in the right seven-eighths. The timeblock pictures f_2 through f_8 continue to shift the vertical edge rightward through A until, in picture 8, A is uniformly 1. Multiplying each timeblock picture $i=1, 2, ..., 9$ by its associated random variable ϕ_i yields, in this particular realization, the stimulus given in Fig. 4b.

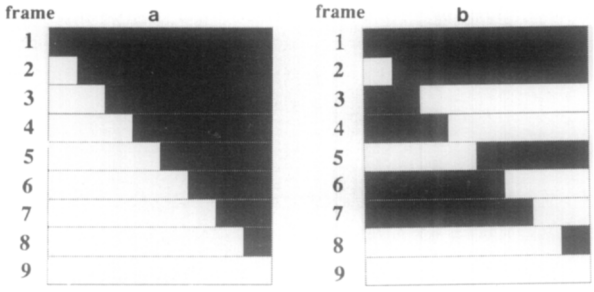

FIG. 4. Edge-driven motion from an ordinary edge and from a binary texture quilt. (a) A rightward moving light–dark edge visible to Fourier and non-Fourier motion systems. Nine entire frames are shown; each frame consists of an area of contrast +1 and area of contrast −1. (b) A realization of the *sidestepping, randomly contrast-reversing vertical edge.* This random stimulus is a texture quilt and hence microbalanced under all purely temporal transformations: that is, its rightward motion would be inaccessible to standard motion-analysis even if this analysis were preceded by an arbitrary, purely temporal transformation. Each frame of (b) was derived from the corresponding frame of (a) by multiplying the entire frame by a random variable that takes the value 1 or −1 with equal probability. The frame random variables are jointly independent. A straightforward way to extract the motion of this texture quilt is to (i) apply a linear filter sensitive to vertical edges, (ii) rectify the filtered output, and (iii) submit the result to standard motion analysis.

The construction of the sidestepping contrast-reversing edge (Fig. 4b) is symmetric to the construction of the traveling contrast-reversal of a random black-or-white vertical bar pattern (J in Fig. 2a). Transposing the x and t dimensions in Fig. 4b gives the xt-cross-section of a random stimulus J (e.g., Fig. 2a). This stimulus exhibits an unusual symmetry between space and time. Whereas the texture quilt of Fig. 4b is microbalanced under all purely temporal transformations, its transpose J (Fig. 2b) is microbalanced under all *purely spatial* transformations. Extracting motion from J requires *temporal* filtering followed by a nonlinearity. This process is essentially different from the process by which motion is extracted from texture quilts (e.g., Figs. 4b, 7a, 7b, and 7c) which requires a *spatial* nonlinearity.

4.4.3. *Stimulus: Oppositely Oriented Static Squarewaves Selected by a Drifting Grating.* Figure 5d shows the four timeblock pictures comprising another binary texture quilt constructed using technique 4.4.1. In Fig. 5a is shown a probabilistically defined sinewave grating, a stimulus whose motion is readily extracted by standard motion-analysis. In Figs. 5b1 and 5b2 are shown static vertical and horizontal squarewave gratings. The stimulus of Fig. 5c is obtained by using Fig. 5a to select between the vertical and horizontal gratings of Figs. 5b1 and 5b2. If the function of Fig. 5a is 1 at a certain point in space-time, the corresponding point in Fig. 5c is assigned the value of the corresponding point in Fig. 5b1; otherwise the point in Fig. 5c is assigned the value of the corresponding point in Fig. 5b2. Although Figs. 5c and 5d look similar, they differ in an important respect: the

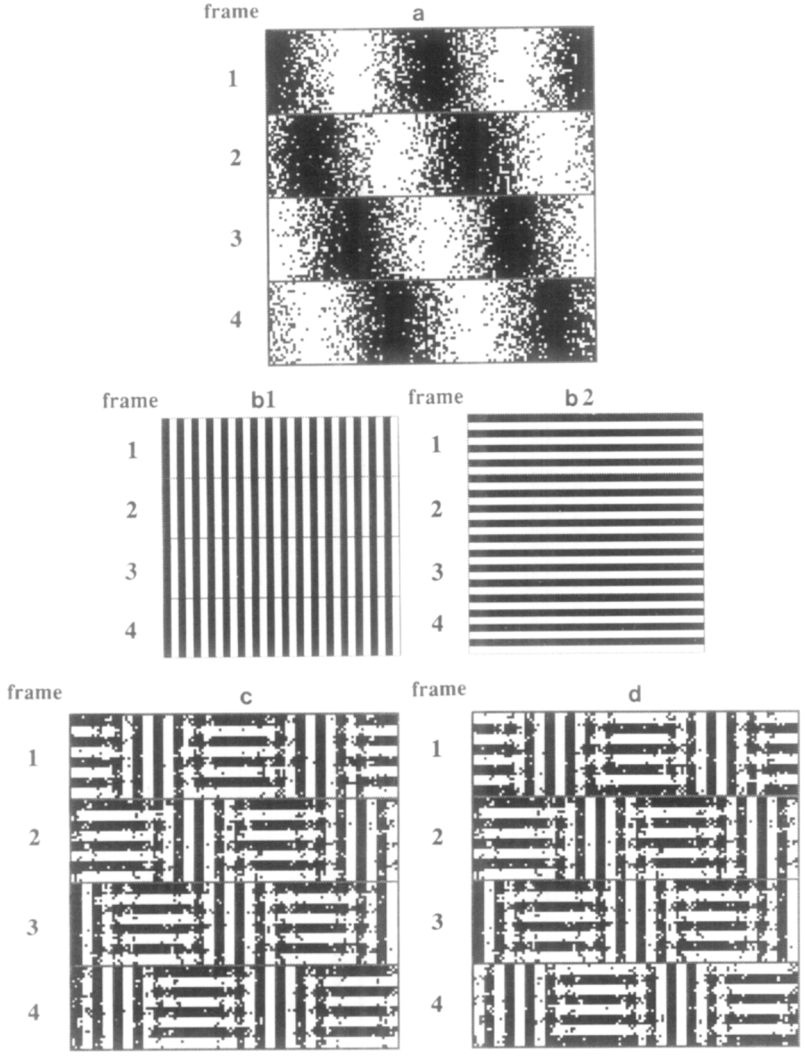

FIG. 5. Orientation-driven non-Fourier motion from a binary texture quilt. (a) A probabilistically defined sinewave grating that steps rightward 90 degrees between frames. The rightward motion in (a) is accessible to all motion detectors. (b1) Four frames of a static, vertical squarewave grating; (b2) Four frames of a static horizontal squarewave grating. (c) A rightward translating texture pattern. For every white point in (a), the corresponding value in (c) is chosen from the vertical squarewave grating in (b1); for every black point in (a), the corresponding value in (c) is chosen from the horizontal square-wave grating in (b2). (c) is not microbalanced; standard motion-analyzers can be designed to detect its motion. (d) A texture quilt. The frames of (d) are derived by multiplying the corresponding frames of (c) by jointly independent random variables, each of which takes the value 1 or -1 with equal probability. The texture quilt (d) is microbalanced under all purely temporal transformations, and therefore its rightward motion is unavailable to any mechanism that applies standard motion analysis to a purely temporal transformation of the visual signal.

stimulus of Fig. 5d is microbalanced under all purely temporal transformations, while that of Fig. 5c is not microbalanced. It is possible to design Fourier mechanisms to detect the motion of Fig. 5c, but not that of Fig. 5d. The critical difference is that the timeblock pictures of Fig. 5d are jointly independent, while those of Fig. 5c are not: Fig. 5d is obtained by randomly reversing the contrasts of the timeblock pictures of Fig. 5c.

4.5. *Sinusoidal Texture Quilts*

It is not difficult to elaborate technique 4.4.1 to a method for constructing quilts involving textures of arbitrarily many contrast values. We illustrate the principle in the construction of quilts comprised of patches of sinusoidal grating.

4.5.1. *A General Technique for Constructing Sinusoidal Texture Quilts.* As in Definition 4.1, let $T = \{t \| t_0 \leqslant t < t_N\}$ be the temporal region of activity, with new timeblocks beginning at times $t_0, t_1, ..., t_{N-1}$. Let A be the spatial region of activity. Associate with timeblocks $i = 0, 1, ..., N-1$, spatial functions W_i, each of which is 0 everywhere outside A, and takes only the values 1 and -1 within A. The stimulus in each time block will be composed of two components characterized by spatial frequencies (ω_i, θ_i) and $(\tilde{\omega}_i, \tilde{\theta}_i)$, respectively, and independent phases $\rho_i, \tilde{\rho}_i$, respectively. Let

$$\omega_0, \theta_0, \tilde{\omega}_0, \tilde{\theta}_0, \omega_1, \theta_1, \tilde{\omega}_1, \tilde{\theta}_1, ..., \omega_{N-1}, \theta_{N-1}, \tilde{\omega}_{N-1}, \tilde{\theta}_{N-1} \tag{41}$$

be integers. Let P be an integer, and let

$$\rho_0, \tilde{\rho}_0, \rho_1, \tilde{\rho}_1, ..., \rho_{N-1}, \tilde{\rho}_{N-1} \tag{42}$$

be jointly independent random variables, each uniformly distributed on the set $\{0, 1, ..., P-1\}$. Then, define the stimulus S as the sum of N component stimuli S_i defined in each timeblock,

$$S = \sum_{i=0}^{N-1} S_i, \tag{43}$$

where, for $i = 0, 1, ..., N-1$, S_i is zero everywhere outside timeblock i; and for all t in timeblock i,

$$S_i[x, y, t] = f_i[x, y] = \begin{cases} \cos(2\pi(\omega_i x + \theta_i y - \rho_i)/P) & \text{if } W_i[x, y] = 1, \\ \cos(2\pi(\tilde{\omega}_i x + \tilde{\theta}_i y - \tilde{\rho}_i)/P) & \text{if } W_i[x, y] = -1, \\ 0 & \text{otherwise.} \end{cases} \tag{44}$$

It is easy to check that S satisfies Definition 4.1(i) and (ii). The joint independence of the random phase variables $\rho_i, \tilde{\rho}_i$, for $i = 0, 1, ..., N-1$ entails Definition 4.1(iii).

It remains to check that S satisfies Definition 4.1(iv). Consider points $\alpha, \beta \in A$. If $W_i[\alpha] \neq W_i[\beta]$, then, as is easily checked, $S[\alpha, t_i]$ and $S[\beta, t_i]$ are independent and identically distributed (each assuming a value from among $\{\cos(2\pi p/P) \| p = 0, 1, ..., P-1\}$ with equal probability). On the other hand, if $W_i[\alpha] = W_i[\beta]$, then the pair $(S[\alpha, t_i], S[\beta, t_i])$ is distributed identically to the pair $(S[\beta, t_i], S[\alpha, t_i])$ as a consequence of the following

LEMMA. *Let* $P \in \mathbf{Z}$, *and let* $\alpha = (\alpha_x, \alpha_y)$, $\beta = (\beta_x, \beta_y)$ *and* $\omega = (\omega_x, \omega_y)$ *all be elements of* $\mathbf{Z}^2$. *Then for any integer* $p \in \{0, 1, ..., P-1\}$, *there exists an integer* $q \in \{0, 1, ..., P-1\}$ *such that* (*writing* $\cdot$ *for dot product*)

$$\cos(2\pi(\omega \cdot \alpha - p)/P) = \cos(2\pi(\omega \cdot \beta - q)/P) \tag{45}$$

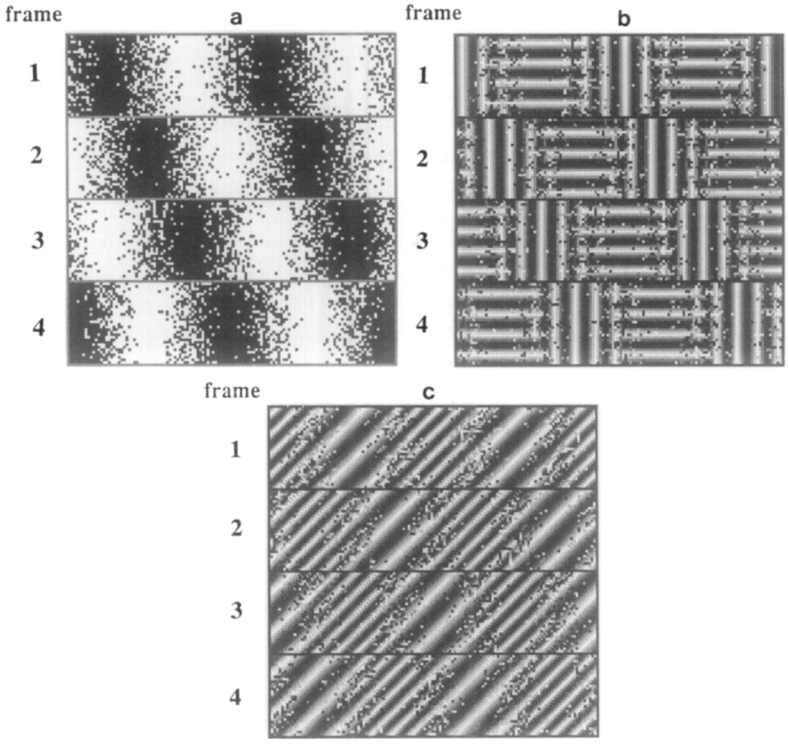

FIG. 6. Sinusoidal texture quilts: Motion driven by differences in *orientation* and in *spatial frequency*. (b) and (c) show realizations of random stimuli, each of which is microbalanced under all purely temporal transformations. Their rightward motion cannot be detected by any mechanism that applies standard motion analysis to a purely temporal transformation of the signal. In each case, the four frames in (a) select between two sinusoidal patterns. The phases of sinusoids are jointly independent across frames and across different-frequency sinusoidal components patched together in the same frame. The sinusoids mixed in (b) differ in orientation, whereas the sinusoids mixed in (c) have the same orientation, but differ in spatial frequency.

and

$$\cos(2\pi(\omega \cdot \beta - p)/P) = \cos(2\pi(\omega \cdot \alpha - q)/P). \tag{46}$$

Proof. As the reader may check, this is true for $q = (\omega \cdot \alpha + \omega \cdot \beta - p)$ modulo P. ▮

Thus, for α, β such that $W_i[\alpha] = W_i[\beta]$, we observe that for any outcome $\rho_i = p$, there exists an equally likely outcome $\rho_i = q$, such that

$$\begin{aligned}&(\cos(2\pi(\omega_i \cdot \alpha - p)/P), \cos(2\pi(\omega_i \cdot \beta - p)/P)\\ &\quad = (\cos(2\pi(\omega_i \cdot \beta - q)/P), \cos(2\pi(\omega_i \cdot \alpha - q)/P)).\end{aligned} \tag{47}$$

We infer that the pair $(S[\alpha, t_i], S[\beta, t_i])$ is distributed identically to the pair $(S[\beta, t_i], S[\alpha, t_i])$.

4.5.2. *Stimulus: Oppositely Oriented Static Sinusoids Selected by a Drifting Grating.* The sinusoidal analog to the binary texture quilt of Fig. 5d is shown in Fig. 6b. In Fig. 6a are shown the functions W_1, W_2, W_3, and W_4 used to select between horizontal and vertical gratings. For this quilt, $\tilde{\omega}_i = \theta_i = 0$, for $i = 1, 2, 3, 4$; and for some integer F (with F/P the number of cycles per pixel), $\omega_i = \tilde{\theta}_i = F$. The texture quilt of Fig. 6b modulates textural orientation across space and time. Alternatively, we can just as easily keep orientation constant and vary spatial frequency.

4.5.3. *Stimulus: Static Sinusoids of Different Spatial Frequencies, Selected by a Drifting Grating.* Figure 6c shows a texture quilt using the sampling functions of Fig. 6a, but setting $\omega_i = \theta_i = 2\tilde{\omega}_i = 2\tilde{\theta}_i$ for $i = 1, 2, \ldots, 4$.

5. What Aspects of Texture Does the Visual System Process for Motion?

In this section, we describe a psychophysical experiment investigating the question of what characteristics of spatial texture are analyzed for motion information by the visual system. Three texture quilts are compared across four different viewing conditions. These conditions comprise a sequence of similar but increasingly challenging motion discrimination tasks.

5.1. *Procedure*

Every texture quilt used in this experiment is comprised of a sequence of jointly independent timeblocks, each lasting 1/30 s. (Each timeblock consists of two identical refreshes at 1/60 s.) Each texture quilt is stochastically periodic with a period of 8 timeblocks: that is, for any integer i, the ith timeblock is identically distributed to the $i+8$th timeblock. Accordingly, we refer to 8 timeblocks of the texture quilt as one *cycle*. The motion elicited by each quilt is carried by a squarewave that selects between two textures, and steps 1/4 cycle on every odd timeblock. The squarewave thus completes one of its four-step cycles in each 8 timeblock cycle of the quilt.

On each trial, a texture quilt moving randomly left or right is presented, and the subject is required to signal (with a button-press) which way the quilt appeared to move. The subject is asked to maintain fixation on a small spot present in the middle of the stimulus throughout the display, and receives feedback after each trial. For each quilt under each viewing condition, the subject performs 100 practice trials followed directly by 100 actual trials. Quilt realizations are jointly independent across trials. The starting phase of the quilt is chosen randomly on each trial.

The Four Viewing Conditions. For a given quilt, the four viewing conditions differ with respect to the number of quilt cycles displayed. In Condition 1, the easiest condition, the subject sees two quilt cycles (each cycle comprised of eight stimulus timeblocks), with each timeblock displayed for 1/30 s. In Conditions 2, 3, and 4, the subject sees 1.5, 1, and 0.5 quilt cycles, respectively.

5.1.1. *Three Quilt Stimuli.* The first quilt (the **F**-quilt) modulates textural spatial frequency as a function of space and time, while keeping orientation constant. The 8 timeblocks comprising one full cycle of the **F**-quilt are shown in Fig. 7a. A second quilt (the **O**-quilt, Fig. 7b) modulates textural orientation as a function of space and time, while keeping spatial frequency constant. A third quilt (the **E**-quilt, Fig. 7c) spatiotemporally modulates texture between jointly independent binary noise and the so-called "even" texture (Julesz, Gilbert, & Victor, 1978).

All stimuli were viewed from 1 m against a mean luminant background. At this distance, each quilt spanned 6.8 horizontal and 3.2 vertical degrees, and the modulating squarewave moved at an average velocity of 12.75 deg/s.

5.1.2. *Why These Three Quilts.* In each of the three quilts, a squarewave with vertical bars is used to modulate between two textures as a function of space and time. The squarewave has a spatial frequency of 0.3 c/deg, and steps 1/4 cycle rightward on every odd timeblock (temporal frequency 3.75 Hz, velocity 12.75 deg/s). We use a 1/4 cycle stepping squarewave to modulate between the two textures comprising each quilt in order to rule out the possibility that the motion elicited by the quilt is being carried by the border between textural regions. That is, the 1/4 cycle stepping squarewave has the advantage that the signal derived from the borders between texture regions is ambiguous in motion content. Given the requirement of 1/4 cycle steps, we changed the particular instantiation of the quilt on even timeblocks (i.e., within steps of the squarewave) in order to spread textural energy broadly in temporal frequency without altering the spatial frequency content of the texture.

It has been previously observed (Green, 1986; Ramachandran, Ginsburg, & Anstis, 1983; Watson & Ahumada, 1983a) that motion is carried more effectively by spatiotemporal variation of textural spatial frequency than by variation of textural orientation. The **F**-quilt and **O**-quilt were chosen to further investigate this claim. The **E**-quilt is of interest because the two textures of which it is composed (jointly independent binary noise and the even texture) have identical second order

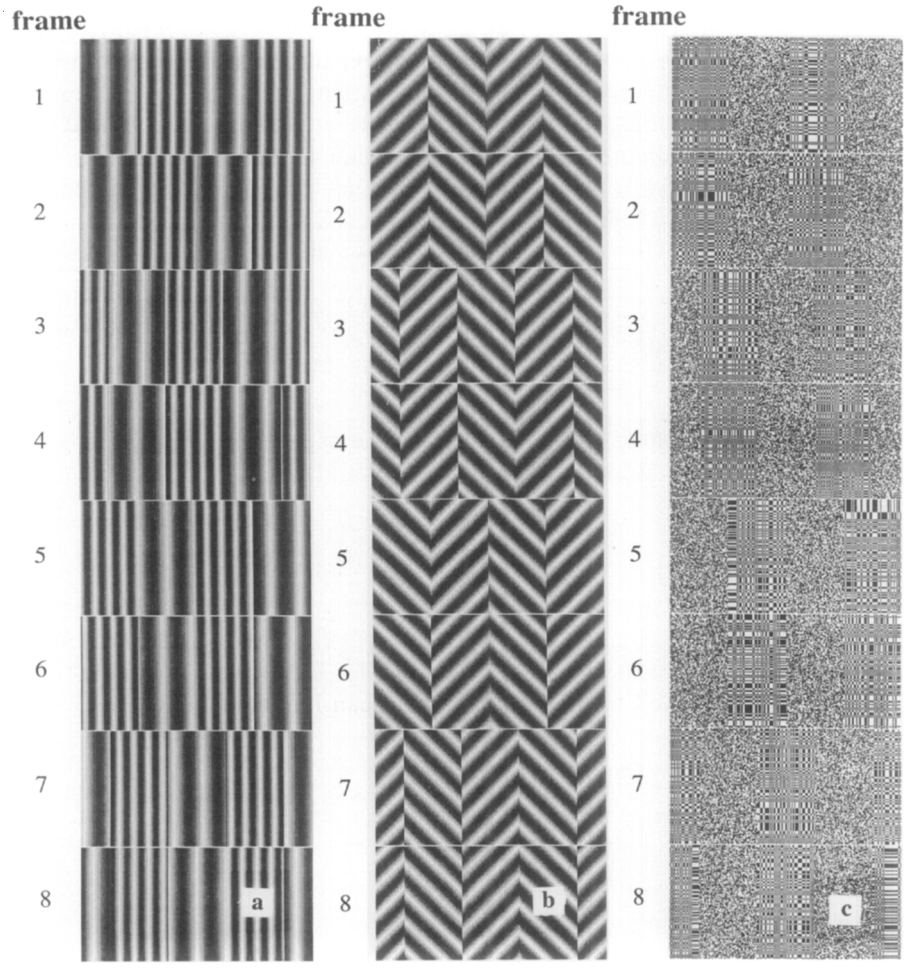

FIG. 7. Three quilts used to study motion carried by modulation of texture spatial frequency, by texture orientation, and by higher order textural characteristics. (a) Eight frames that comprise one cycle of the **F**-quilt. Motion is generated by a squarewave modulation of textural spatial frequency. The squarewave grating selects between vertical sinusoidal gratings of spatial frequency 1.2 and 2.4 c/deg. The texture-modulating squarewave is 0.3 c/deg, and steps 1/4 cycle rightward on every odd frame. Every even frame is independent of and distributed identically to the preceding frame. Presentation proceeds at the rate of 30 frames/s. This gives the texture-modulating squarewave a temporal frequency of 3.75 Hz and a mean velocity of 25 deg/s. (b) Eight frames that comprise one cycle of the **O**-quilt. In the **O**-quilt, textural orientation is modulated by the same squarewave used to modulate spatial frequency in the **F**-quilt. The **O**-quilt squarewave selects between oppositely oriented sinusoidal gratings that have a spatial frequency of 2.8 c/deg. (c) Eight frames that comprise one cycle of the **E**-quilt. In the **E**-quilt, the texture-modulating squarewave selects between jointly independent binary noise and an even texture (Julesz, Gilbert, & Victor, 1978). Despite the evident difference between these two textures, every time-independent linear filter has the same expected power for both textures. Thus, if motion-from-texture resulted from applying a simple squaring transformation to the output of a spatial linear filter and submitting the result to standard motion analysis, the motion of the **E**-quilt would be invisible.

statistics. That is, the joint distribution of any given pair of points in space is the same under both the component textures of the **E**-quilt. This means that, despite the obvious difference in appearance between the component textures, the expected energy in the response of any given spatial linear filter is the same for both component textures. If the pointwise nonlinearity applied to the output of the spatial linear filter prior to motion analysis were simple squaring, it would be impossible to detect the motion of the **E**-quilt.

Victor and Conte (1990) studied apparent motion elicited by **E**-quilts, and noted that it is much weaker than motion elicited by comparable stimuli (also texture quilts) that modulate between textures differing in spatial frequency. Our experiment confirms this finding.

5.2. *Results*

Two subjects participated in the study, CC (the experimenter) and GA (naive). The results for CC are shown in Fig. 8 bottom, and those for GA are shown in

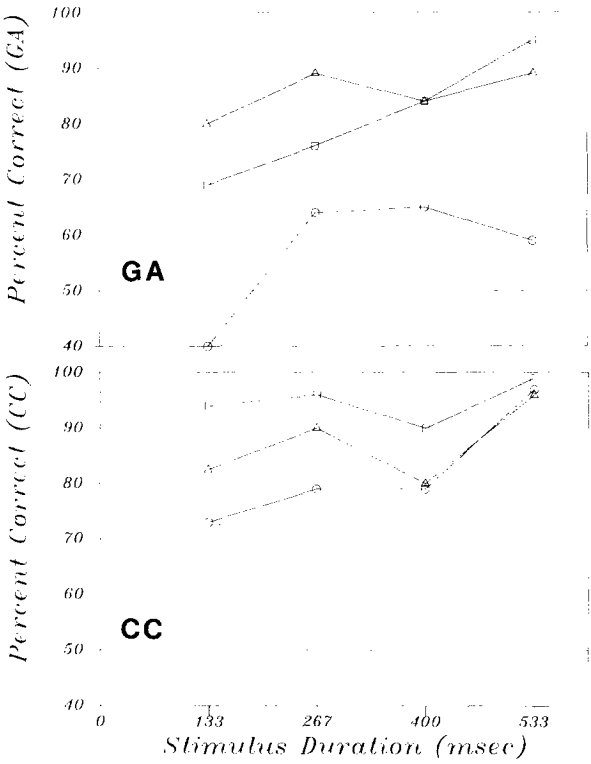

FIG. 8. The percent of correct direction-of-motion judgments to the **F**-quilt, the **O**-quilt, and the **E**-quilt as a function of stimulus duration. The panels show data for subjects CC and GA, respectively. Each data point is the mean of 100 judgments. (Squares) **F**-quilt; (triangles) **O**-quilt; (circles) **E**-quilt. The stimulus durations of 133, 266, 400, and 533 ms, correspond to stimulus presentations of 0.5, 1, 1.5, and 2 quilt cycles.

Fig. 8 top. Note first that both subjects were able to reliably discriminate left/right motion in all three stimuli although subject GA failed with the **E**-quilt at the briefest exposure. The two subjects performed comparably well at motion direction discrimination of the **O**-quilt, but CC was much better than GA at detecting the motion of both the **F**-quilt and the **E**-quilt. Subject CC was better at detecting the motion of the **F**-quilt than the **O**-quilt; the reverse was true of subject GA.

It is possible that these performance differences reflect a genuine differences in the perceptual apparatus of the two subjects. However, we cannot rule out the possibility that the better performance of subject CC is due merely to his vastly greater experience with motion perception tasks of this sort.

5.3. *Discussion*

Many of the models proposed to explain rapid, preattentive segregation of spatial textures (Beck, Sutter, & Ivry, 1987; Bergen & Adelson, 1988; Caelli, 1985; Malik & Perona, 1989; Sutter, Beck, & Graham, 1989) can easily be adapted to deal with the motion displayed by texture quilts. The texture segregation models in this class typically subject the visual input function to a linear transformation (a "texture grabber") followed by a pointwise nonlinearity (such as a rectifier or thresholder) to indicate the presence or absence of the texture. Such models propose that two contiguous textural regions would generate a perceptual boundary if the visual system were equipped with a linear filter that is differentially tuned to one of the textures.

An analogous mechanism to detect the motion of texture quilts, suggested by the current experiment and the work of Victor and Conte (1990), (i) convolves the input stimulus with a spatial texture-grabbing filter tuned to the moving texture, then (ii) squares the output of the filter, to transform regions of high energy filter output into regions of high average value, and (iii) subjects the rectified output to standard motion analysis. However, the transformation applied in steps (i) and (ii) does not distinguish between the two textures comprising the **E**-quilt, and therefore fails to account for the good performance with the **E**-quilt. A simple modification to deal with texture segregation and motion perception of the **E**-quilt is to assume some other post-filter rectification operation than the squaring operation. It is quite easy to choose a linear filter in combination with a post-filter rectifier (other than the squaring operation) that will segregate the random and even textures (e.g., Julesz & Bergen, 1983). The current experiment does not specifically indicate the kind of rectification that might be involved.

What sorts of filters are available to the visual system to compute motion from texture? For example, Daugman (1985) points out that (i) Gabor filters provide an optimal tradeoff between resolution in the space and spatial frequency domains, and (ii) many investigators note that simple cells in cat striate cortex are well modeled by oriented Gabor filters (e.g., Andrews & Pollen, 1979; DeValois, DeValois, & Yund, 1979; Wilson & Sherman, 1976). Are the linear filters that serve motion-from-texture computations Gabor-like cortical simple cells? The theory

reported here provides a tool, and the demonstration experiments illustrate how it might be used to answer such questions.

6. Summary

The main contributions of this paper are to (i) introduce the notion of a random stimulus *microbalanced under all pointwise transformations*, (ii) provide necessary and sufficient conditions for a random stimulus to be of this sort, (iii) use this result to construct apparent motion stimuli called *texture quilts* that are microbalanced under all purely temporal transformations, and (iv) show that subjects can reliably discriminate the motion direction of three kinds of texture quilts.

Texture quilts provide a flexible array of tools for studying motion perception that is truly mediated by spatiotemporal modulation of spatial texture without contamination by mechanisms responsive to the motion extracted directly by standard analysis or motion extracted by standard analysis of any purely temporal transformation of the stimulus.

Acknowledgments

The research reported here was supported by USAF Life Science Directorate, Visual Information Processing Program Grants 85-0364 and 88-0140.

References

Adelson, E. H., & Bergen, J. (1985). Spatiotemporal energy models for the perception of motion. *Journal of the Optical Society of America A*, **2**(2), 284–299.

Adelson, E. H., & Bergen, J. (1986). The extraction of spatio-temporal energy in human and machine vision. *Proceedings of the IEEE Workshop on Motion: Representation and Analysis*, 151–155.

Andrews, B. W., & Pollen, D. A. (1979). Relationship between spatial frequency selectivity and receptive field profile of simple cells. *Journal of Physiology (London)*, **287**, 163–176.

Anstis, S. M. (1970). Phi movement as a subtraction process. *Vision Research*, **10**, 1411–1430.

Baker, C. L., & Braddick, O. (1982a). Does segregation of differently moving areas depend on relative or absolute displacement. *Vision Research*, **22**, 851–856.

Baker, C. L., & Braddick, O. (1982b). The basis of area and dot number effects in random dot motion perception. *Vision Research*, **22**, 1253–1260.

Beck, J., Sutter, A., & Ivry, R. (1987). Spatial frequency channels and perceptual grouping in texture segregation. *Computer Vision, Graphics, and Image Processing*, **37**, 299–325.

Bell, H. H., & Lappin, J. S. (1979). The detection of rotation in random dot patterns. *Perception and Psychophysics*, **26**, 415–417.

Bergen, J. R., & Adelson, E. H. (1988). Early vision and texture perception. *Nature*, **333**(6171), 363–364.

Bowne, S. F., McKee, S. P., & Glaser, D. A. (1989). Motion interference in speed discrimination. *Journal of the Optical Society of America A*, **6**(7), 1112–1121.

Braddick, O. (1973). The masking of apparent motion in random-dot patterns. *Vision Research*, **13**, 355–359.

BRADDICK, O. (1974). A short-range process in apparent motion. *Vision Research*, **14**, 519–527.

CAELLI, T. (1985). Three processing characteristics of visual texture segmentation. *Spatial Vision*, **1**(1), 19–30.

CAVANAGH, P. (1988). Motion: The long and the short of it. Presented at *Conference on Visual From and Motion Perception: Psychophysics, Computation, and Neural Networks* (Meeting dedicated to the memory of the late Kvetoslav Prazdny). Boston University, MA, March 5, 1988.

CAVANAGH, P., ARGUIN, M., & VON GRUNAU, M. (1989). Interattribute apparent motion. *Vision Research*, **29**(9), 1197–1204.

CHANG, J. J., & JULESZ, B. (1983a). Displacement limits, directional anisotropy and direction versus form discrimination in random dot cinematograms. *Vision Research*, **23**, 639–646.

CHANG, J. J., & JULESZ, B. (1983b). Displacement limits for spatial frequency random-dot cinematograms in apparent motion. *Vision Research*, **23**, 1379–1386.

CHANG, J. J., & JULESZ, B. (1985). Cooperative and non-cooperative processes of apparent movement of random dot cinematograms. *Spatial Vision*, **1**(1), 39–45.

CHUBB, C., & SPERLING, G. (1987). Drift-balanced random stimuli: A general basis for studying non-Fourier motion perception. *Investigative Ophthalmology and Visual Science*, **28**, 233.

CHUBB, C., & SPERLING, G. (1988). Drift-balanced random stimuli: A general basis for studying non-Fourier motion perception. *Journal of the Optical Society of America A*, **5**(11), 1986–2007.

DAUGMAN, J. G. (1985). Uncertainty relation for resolution in space, spatial frequency, and orientation optimized by two-dimensional visual cortical filters. *Journal of the Optical Society of America A*, **2**(7), 1160–1169.

DERRINGTON, A. M., & BADCOCK, D. R. (1985). Separate detectors for simple and complex grating patterns? *Vision Research*, **25**, 1869–1878.

DERRINGTON, A. M., & HENNING, G. B. (1987). Errors in direction-of-motion discrimination with complex stimuli. *Vision Research*, **27**, 61–75.

DEVALOIS, K. K., DEVALOIS, R. L., & YUND, E. W. (1979). Responses of striate cortical cells to grating and checkerboard patterns. *Journal of Physiology (London)*, **291**, 483–505.

VAN DOORN, A. J., & KOENDERINK, J. J. (1984). Spatiotemporal integration in the detection of coherent motion. *Vision Research*, **24**, 47–54.

DOSHER, BARBARA A., LANDY, M. S., & SPERLING, G. (1989). Ratings of kinetic depth in multi-dot displays. *Journal of Experimental Psychology: Human Perception and Performance*, **15**, 116–425.

GREEN, M. (1986). What determines correspondence strength in apparent motion. *Vision Research*, **26**, 599–607.

JULESZ, B. (1971). *Foundations of cyclopean perception*. Chicago: Univ. of Chicago Press.

JULESZ, B., & BERGEN, J. R. (1983). Textons, the fundamental elements in preattentive vision and perception of textures. *Bell Systems Technical Journal*, **62**(6), 1619–1645.

JULESZ, B., GILBERT, E., & VICTOR, J. D. (1978). Visual discrimination of textures with identical third-order statistics. *Biological Cybernetics*, **31**, 137–140.

LAPPIN, J. S. (1989). Personal communication, June 20.

LAPPIN, J. S., & BELL, H. H. (1972). Perceptual differentiation of sequential visual patterns. *Perception and Psychophysics*, **12**, 129–134.

LELKINS, A. M. M., & KOENDERINK, J. J. (1984). Illusory motion in visual displays. *Vision Research*, **24**, 1083–1090.

MALIK, J., & PERONA, P. (1989). *A computational model of texture perception* (Computer Science Division (EECS) Report No. UCB/CSD 89/491). Berkeley: University of California.

MARR, D. & ULLMAN, S. (1981), Direction selectivity and its use in early visual processing, *Proc. R. Soc. London, Ser. B*, **211**, 151–180.

NAKAYAMA, K., & SILVERMAN, G. (1984). Temporal and spatial characteristics of the upper displacement limit for motion in random dots. *Vision Research*, **24**, 293–300.

PANTLE, A., & TURANO, K. (1986). Direct comparisons of apparent motions produced with luminance, contrast-modulated (CM), and texture gratings. *Investigative Ophthalmology and Visual Science*, **27**(3), 141.

PETERSIK, J. T., HICKS, K. I., & PANTLE, A. J. (1978). Apparent movement of successively generated subjective figures. *Perception*, **7**, 371–383.

RAMACHANDRAN, V. S., & ANSTIS, S. M. (1983). Displacement thresholds for coherent apparent motion in random dot-patterns. *Vision Research*, **23**, 1719–1724.

RAMACHANDRAN, V. S., GINSBURG, A., & ANSTIS, S. M. (1983). Low spatial frequencies dominate apparent motion. *Perception*, **12**, 457–461.

RAMACHANDRAN, V. S., RAO, V. M., & VIDYASAGAR, T. R. (1973). Apparent movement with subjective contours. *Vision Research*, **13**, 1399–1401.

VAN SANTEN, J. P. H., & SPERLING, G. (1984). A temporal covariance model of motion perception. *Journal of the Optical Society of America A*, **1**, 451–473.

VAN SANTEN, J. P. H., & SPERLING, G. (1985). Elaborated Reichardt detectors. *Journal of the Optical Society of America A*, **2**(2), 300–321.

SHAPLEY, R., & ENROTH-CUGELL, C. (1984). Visual adaptation and retinal gain controls. *Progress in Retinal Research*, **3**, 263–346, 1984.

SPERLING, G. (1976). Movement perception in computer-driven visual displays. *Behavior Research Methods and Instrumentation*, **8**, 144–151.

SUTTER, A., BECK, J., & GRAHAM, N. (1989). Contrast and spatial variables in texture segregation: Testing a simple spatial-frequency channels model. *Perception and Psychophysics*, **46**(4), 312–332.

TURANO, K., & PANTLE, A. (1989). On the mechanism that encodes the movement of contrast variations: Velocity discrimination. *Vision Research*, **29**(2), 207–221.

ULLMAN, S. (1979). *The Interpretation of Visual Motion*. Cambridge, MA: MIT Press.

VICTOR, J. D., & CONTE, M. M. (1990). Motion mechanisms have only limited access to form information. *Vision Research*, **30**(2), 289–301.

WATSON, A. B., & AHUMADA, A. J., JR. (1983a). A linear motion sensor. *Perception*, **12**, A17.

WATSON, A. B., & AHUMADA, A. J., JR. (1983b). *A look at motion in the frequency domain*. NASA Technical Memorandum 84352.

WATSON, A. B., & AHUMADA, A. J., JR. (1985). A model of human visual-motion sensing. *Journal of the Optical Society of America A*, **2**(2), 322–342.

WATSON, A. B., AHUMADA, A. J., & FARRELL, J. E. (1986). The window of visibility: A psychophysical theory of fidelity in time-sampled motion displays. *Journal of the Optical Society of America A*, **3**(3), 300–307.

WILSON, J., & SHERMAN, S. (1976). Receptive field characteristics of neurones in cat striate cortex: Changes with visual field eccentricity. *Journal of Neurophysiology*, **39**, 512–533.

RECEIVED: February 8, 1989